This Research Contribution is in Commemoration of the Life and Science of I. M. Kolthoff (1894–1993).

Scanning Electrochemical Microscopy. 24. Enzyme Ultramicroelectrodes for the Measurement of Hydrogen Peroxide at Surfaces

Benjamin R. Horrocks

Department of Chemistry and Biochemistry, The University of Texas at Austin, Austin, Texas 78712

David Schmidtke and Adam Heller*

Department of Chemical Engineering, The University of Texas at Austin, Austin, Texas 78712

Allen J. Bard*

Department of Chemistry and Biochemistry, The University of Texas at Austin, Austin, Texas 78712

Hydrogen peroxide sensing microelectrodes for scanning electrochemical microscopy (SECM) have been developed and used to measure hydrogen peroxide in the diffusion layer during electrochemical reduction of oxygen on gold and carbon electrodes. These microelectrode biosensors were also used to detect immobilized glucose oxidase through the production of hydrogen peroxide during enzymatic oxidation of glucose. Images of hydrogen peroxide concentration profiles near a platinum microdisk during catalytic decomposition of peroxide and in the diffusion layer of a carbon–platinum composite electrode during oxygen reduction are presented. The factors limiting the spatial resolution (tens of micrometers) and potential applications of the technique are discussed.

INTRODUCTION

In scanning electrochemical microscopy (SECM), an ultramicroelectrode (UME) tip is scanned over the surface of a sample. Topographic and chemical information about the surface and electrochemical processes in the diffusion layer can be obtained from the faradaic current at the UME.[1-3] Commonly, a reversible redox mediator is used and the UME is poised at a potential where the reaction at the tip is diffusion controlled. At such a potential, the tip current is determined by the rate of mass transfer to the tip, which is a known function of the tip-to-sample separation.[4] The current decreases near an insulating surface and increases near a conductor. Insulators, conductors, and samples containing both insulating and conducting regions have been imaged.[5,6] Chemical information about the surface can be obtained by an appropriate choice of mediator. Thus, when the kinetics of regeneration of the mediator at a particular site are slow, the distribution of the slow sites can be mapped.[7,8] Although many chemical systems can be investigated in this way (metals, polymers, semiconductors, oxides, immobilized enzymes),[2,3] the scope of the technique is limited to systems that can be probed by redox mediators. Thus these SECM techniques, like voltammetric methods, have a limited degree of chemical selectivity. Several laboratories have developed potentiometric UME for use in SECM[9,10] and localized measurements of corrosion.[11,12] Potentiometric microelectrodes are also widely used in biology for intracellular measurements of ion concentrations.[13] The use of potentiometry in SECM should allow the monitoring of local pH and halide and alkali metal ion concentrations. In this paper, we show that the scanning tip can be made selective by "electrically wiring" an enzyme to the UME via a cross-linked redox polymer to produce an electrochemical biosensor.

Many different designs for enzyme UMEs have been reported, including physical entrapment on platinum,[14-16] conducting organic salts,[17] covalent attachment using biotin–avidin,[18,19] and immobilization in cross-linked redox polymers.[20] The SECM tips were made by electrically wiring horseradish peroxidase to a carbon electrode via a cross-linked redox polymer (shown in Figure 1).[21,22] The redox polymer

* Author to whom correspondence should be addressed.

(1) Engstrom, R. C.; Pharr, C. M. *Anal. Chem.* **1989**, *61*, 1099A.
(2) Bard, A. J.; Fan, F.-R. F.; Pierce, D. T.; Unwin, P. R.; Wipf, D. O.; Zhou, F. *Science* **1991**, *254*, 68.
(3) Bard, A. J.; Denuault, G.; Lee, C.; Mandler, D.; Wipf, D. O. *Acc. Chem. Res.* **1990**, *23*, 357.
(4) Kwak, J.; Bard, A. J. *Anal. Chem.* **1989**, *61*, 1221.
(5) Lee, C.; Miller, C. J.; Bard, A. J. *Anal. Chem.* **1991**, *63*, 78.
(6) Wipf, D. O.; Bard, A. J.; Tallmann, D. E. *Anal. Chem.* **1993**, *65*, 1373.
(7) Wipf, D. O.; Bard, A. J. *J. Electrochem. Soc.* **1991**, *138*, L4.
(8) Engstrom, R. C.; Small, B.; Kattan, L. *Anal. Chem.* **1992**, *64*, 241.
(9) Denuault, G.; Troise-Frank, M. H.; Peter, L. M. *Faraday Discuss. Chem. Soc.* **1992**, *No. 94*, 23.
(10) Horrocks, B. R.; Mirkin, M. V.; Pierce, D. T.; Bard, A. J.; Nagy, G.; Toth, K. *Anal. Chem.* **1993**, *65*, 1213.
(11) Luo, J. L.; Lu, Y. C.; Ives, M. B. *J. Electroanal. Chem.* **1992**, *326*, 51.
(12) Davis, J. A. *NACE Localized Corros.* **1974**, *3*, 168.
(13) Ammann, D. *Ion Selective Microelectrodes: Principles, Design and Application*; Springer: New York, 1986.
(14) Abe, T.; Lau, Y. Y.; Ewing, A. G. *J. Am. Chem. Soc.* **1991**, *113*, 7421.
(15) Ikariyama, Y.; Yamauchi, S.; Aizawa, M.; Yukiashi, T.; Ushioda, H. *Bull. Chem. Soc. Jpn.* **1988**, *61*, 3525.
(16) Cronenberg, C. C. H.; van den Heuvel, J. C. *Biosens. Bioelectron.* **1991**, *6*, 255.
(17) Kawagoe, J. L.; Niehaus, D. E.; Wightman, R. M. *Anal. Chem.* **1991**, *63*, 2961.
(18) Pantano, P.; Morton, T. H.; Kuhr, W. G. *J. Am. Chem. Soc.* **1991**, *113*, 1832.
(19) Pantano, P.; Kuhr, W. G. *Anal. Chem.* **1993**, *65*, 617, 623.
(20) Pishko, M.; Michael, A. C.; Heller, A. *Anal. Chem.* **1991**, *63*, 2268.
(21) Heller, A. *Acc. Chem. Res.* **1990**, *23*, 128.

0003-2700/93/0365-3605$04.00/0

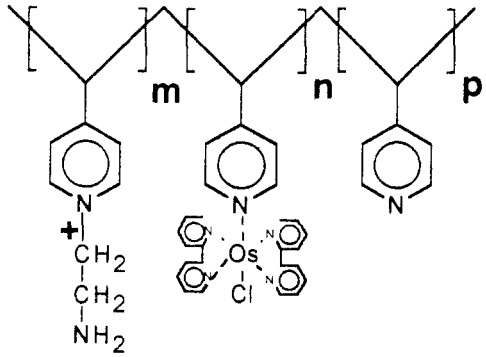

Figure 1. Structure of the osmium redox polymer (1) used in the preparation of the hydrogen peroxide biosensors.

provides an electron diffusion path from the carbon electrode to the reaction center of the enzyme. A cathodic current flows when hydrogen peroxide is reduced to water by the enzyme, the oxidized enzyme is reduced by Os^{2+} centers of the polymer, and the resulting Os^{3+} sites are electroreduced through electron transport via the polymer from the electrode. The advantages of this type of biosensor include high current density and insensitivity to oxygen concentration.[20] We chose a hydrogen peroxide sensing tip because hydrogen peroxide is frequently produced in enzymatic and electrochemial systems through the reduction of oxygen.

The reduction of oxygen on metals has been extensively studied because of its importance as the cathode reaction in fuel cells.[23,24] In protic solvents, the final reduction product can be water or hydrogen peroxide, depending on the electrode material. For an efficient fuel cell, it is desirable that oxygen is reduced directly to water in a four-electron reaction at low overpotential rather than in the two-electron reaction to hydrogen peroxide, and a great deal of effort has been put into designing electrocatalysts to achieve this.[24-26] The activity of these electrodes and the relative contribution of the two-electron and four-electron paths is often examined by rotating ring–disk electrode (RRDE) techniques.[27] In this approach, the disk is fabricated from the catalyst of interest, and a platinum ring is used to detect hydrogen peroxide by amperometric oxidation. Because the reduction of hydrogen peroxide is very sensitive to the cleanliness of the surface,[23,24] H_2O_2 is detected at a platinum ring held at a high positive potential, e.g., +1.0 V, sufficient to oxidize hydrogen peroxide. However, a hydrogen peroxide biosensor is much more selective than a platinum electrode held at +1.0 V and therefore should be applicable to systems where the presence of other electroactive compounds would prevent the use of platinum electrodes.

Hydrogen peroxide is also a byproduct of the reactions of many enzymatic oxidations where the oxidized form of the enzyme is regenerated by reaction of the reduced enzyme with oxygen.[28] Although immobilized oxidoreductases have been studied successfully by SECM with simple redox mediators,[29] it would also be interesting to be able to study these reactions with the usual biological substrate of the enzyme, oxygen.

The aim of this paper is to show that amperometric biosensors can be employed as the tip in SECM. Examples of the information that they can provide in studies of electrochemical and enzymatic oxygen reduction are presented. The advantages and disadvantages of the technique compared to RRDE and simple voltammetric SECM techniques are also discussed. Images of the distribution of catalytic activity on model surfaces are shown, and the technique is compared to other methods of imaging electrochemical activity, such as SECM with voltammetric microelectrodes and fluorescence imaging.[30]

THEORY

As in any scanning probe microscopy, it is necessary to determine the absolute tip-to-sample distance in order to bring the tip close to the surface and to extract quantitative information about concentrations near the surface. In SECM with redox mediators, this is very conveniently done by monitoring the faradaic current at the UME tip as it approaches the surface.[4] This approach is not possible with the biosensor tips used in this paper for two reasons. First, it it undesirable to add a redox mediator to the solution, because this could perturb the chemistry of the system. Second, the rate of diffusion of redox mediators in polymers is slower than in aqueous solutions, and the faradaic current for a redox mediator at the tip may be limited by diffusion through the polymer film. The tip current would therefore be insensitive to the rate of diffusion in the solution and hence to the tip-to-sample distance. However, a modification of the procedure is possible. By applying a high-frequency alternating potential to the tip, the solution resistance between the tip and the auxiliary electrode can be measured. As the tip approaches an insulator, the solution resistance increases because the surface partially blocks some of the pathways for ions to travel between the tip and the auxiliary electrode. A similar effect is applied in scanning ion conductance microscopy.[31] Near a conducting surface, the measured resistance decreases as the tip approaches the surface, because the alternating current can now flow through the conductor; this applies equally whether the conducting sample is used as the auxiliary electrode or is simply left at open circuit. The dependence of the solution resistance on tip-to-surface separation can be calculated with two assumptions: (i) the impedance of the cell can be approximated by a simple series combination of the tip double-layer capacitance and the solution resistance, and (ii) the contribution of the polymer film on the tip to the resistance is either constant or negligible. For a conductive substrate, the measured capacitance will include a contribution from the substrate. At small tip–surface separations, only the part of the substrate underneath the tip is active and the capacitance of this region may be of the same order as the tip double-layer capacitance. However, this effect was found to be within the accuracy of our experimental data and therefore no correction for this effect was applied.

The computation of the solution resistance between a disk electrode and an auxiliary electrode at infinity has been carried out by Newman by solving the Laplace equation for the potential distribution.[32] The equivalent problem for the

(22) Heller, A. *J. Phys. Chem.* **1992**, *96*, 3579.
(23) Hoare, J. P. In *Encyclopedia of Electrochemistry of the Elements*; Bard, A. J., Ed.; Marcel Dekker: New York, 1974; Vol. II, pp 305–337.
(24) Yeager, E. *Electrochim. Acta* **1984**, *29*, 1527.
(25) Karaman, R.; Jeon, S.; Almarsson, O.; Bruice, T. C. *J. Am. Chem. Soc.* **1992**, *114*, 4899.
(26) Collman, J. P.; Denisevich, P.; Konai, Y.; Marroco, M.; Koval, C.; Anson, F. C. *J. Am. Chem. Soc.* **1980**, *102*, 6027.
(27) Durand, R. R., Jr.; Bencosme, C. S.; Collmann, J. P.; Anson, F. C. *J. Am. Chem. Soc.* **1983**, *105*, 2710.
(28) Dixon, M.; Webb, E. C. *Enzymes*; Academic Press: New York, 1979.
(29) Pierce, D. T.; Unwin, P. R.; Bard, A. J. *Anal. Chem.* **1992**, *64*, 1795.
(30) Engstrom, R. C.; Ghaffari, S.; Qu, H. *Anal. Chem.* **1992**, *64*, 2525.
(31) Hansma, P. K.; Drake, B.; Marti, O.; Gould, S. A. C.; Prater, C. B. *Science* **1989**, *243*, 641.
(32) Newman, J. *J. Electrochem. Soc.* **1966**, *113*, 501.

geometry of SECM can be formulated by the following equations.

$$\nabla^2\phi = 0 \quad (1)$$

with the boundary conditions

$$j = -\kappa\nabla\phi \quad \text{in the solution} \quad (2)$$

$$\phi = \text{const} \quad \text{at a conducting sample–auxiliary electrode} \quad (3)$$

$$\phi = 0 \quad \text{at the tip} \quad (4)$$

$$j = 0 \quad \text{at insulating surfaces and the glass tip sheath} \quad (5)$$

The above equations apply to both dc resistance experiments with a redox couple present and ac experiments in inert electrolyte, as long as ϕ is taken as the alternating part of the potential in the latter case. These equations are strictly analogous to Fick's equation for amperometric SECM at steady state.

$$\nabla^2 c = 0 \quad (6)$$

with the boundary conditions

$$i_T = -nFD\nabla c \quad \text{in the solution} \quad (7)$$

$$c = \text{const} \quad \text{at a conducting sample surface} \quad (8)$$

$$c = 0 \quad \text{at the tip} \quad (9)$$

$$i_T = 0 \quad \text{at insulating surfaces and the glass tip sheath} \quad (10)$$

This analogy has also been pointed out for the calculation of the uncompensated resistance at a UME in bulk solution.[33,34] Using this analogy and normalizing the distance scale by the tip radius, a, we obtain the following expression for the variation of solution resistance with the tip-to-surface separation:

$$R(\infty)/R(d) = i_T(d)/i_{T,\infty} \quad (11)$$

where $i_T(d)$ and $R(d)$ are the feedback current and solution resistance at a normalized tip-to-surface separation of d (in units of tip radius a). This implies that the (decreasing) conductance as the tip approaches an insulator shows the same distance dependence as that of the current in SECM. A similar equivalence exists for the conductance and current with a conductive substrate. Since the distance dependence of the feedback diffusion current is already known,[4] all that remains is to show how the contribution of the solution resistance can be separated from the capacitive contribution to the impedance of the tip.

When the tip–auxiliary electrode cell can be represented by a simple series RC equivalent circuit, the in-phase and quadrature components of the current are

$$i_{0°} = \frac{\omega^2 c_{dl}^2 RV}{1 + \omega^2 c_{dl}^2 R^2} \quad (12)$$

$$i_{90°} = \frac{\omega c_{dl} V}{1 + \omega^2 c_{dl}^2 R^2} \quad (13)$$

where ω, c_{dl}, R, and V are the angular frequency, tip double-layer capacitance, solution resistance, and magnitude of the applied ac voltage, respectively. The normalized solution resistance in eq 11 can then be calculated using

$$\omega c_{dl} R(d) = i_{0°}(d)/i_{90°}(d) \quad (14)$$

After normalizing this by the value of resistance at large distances, $R(\infty)$ (i.e., distances greater than a few radii), a plot of normalized conductance, $R(\infty)/R(d)$, vs distance, d, can be constructed. These data can then be fit to the theory for feedback diffusion in SECM ($i_T(d)/i_{T,\infty}$ vs d) to determine the absolute tip-to-surface distance.

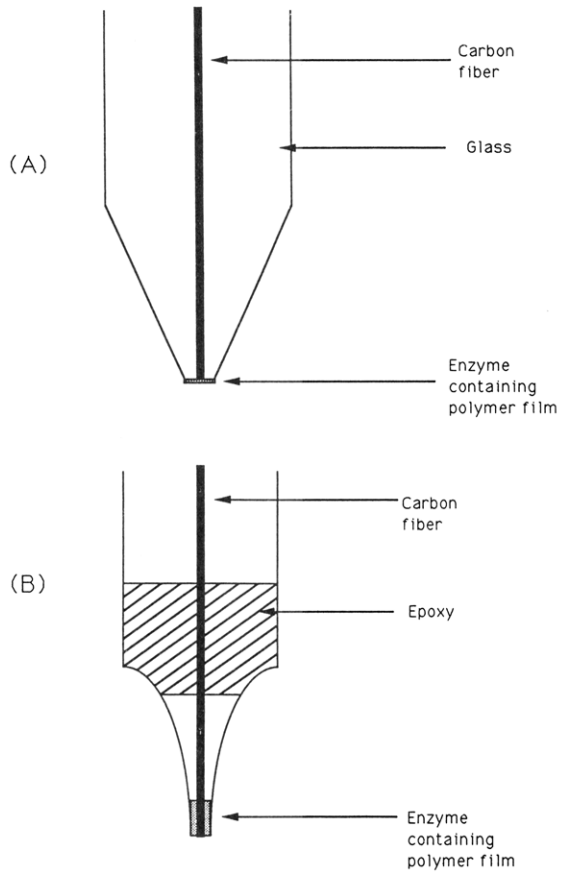

Figure 2. Schematics of the two types (A and B) of hydrogen peroxide sensing microelectrodes used.

EXPERIMENTAL SECTION

Microelectrode Fabrication. Carbon microelectrodes of two different geometries were prepared for use as amperometric biosensors. These are referred to as type A (microdisk) and type B (microcylinder) electrodes.

Type A electrodes (Figure 2A) were prepared by heat sealing 11- or 8-μm-diameter carbon fibers (Amoco Performance Products, Greenville, SC) in 2-mm-o.d. Pyrex capillaries. The tip of the electrode was then beveled to produce an SECM tip, as described previously.[4] The resulting tip geometry was an inlaid microdisk electrode with a ratio of glass sheath diameter to carbon fiber diameter, denoted as RG, of ca. 2–3.

The carbon microdisk was then coated with the electrically wired enzyme. The coating solution contained redox polymer 1, enzyme (horseradish peroxidase), and cross-linker [poly(ethylene glycol) (MW 400) diglycidyl ether] in a weight ratio of 6.2:3.9:1. The tip of the electrode was brought into contact with a drop of the coating solution using a micromanipulator and then withdrawn. The solution was allowed to dry and form a roughly 1-μm-thick film (estimated by optical microscopy) coating the surface of the tip. The film was cured at ambient temperature in air for a minimum of 2 days.

Type B electrodes (Figure 2B) were fabricated in a manner similar to a previously published procedure for glucose-sensing microelectrodes.[20] A 7-μm-diameter carbon fiber was inserted into a 2-mm-o.d. borosilicate glass tube, and the tube was pulled on a micropipet puller (Narishige Model PB-7) to yield a glass tip of approximately 20-μm o.d. The glass tip was then partially filled with a low-viscosity epoxy, leaving a microcylinder as the electrode surface, and was cured at 70 °C overnight. The tip was then polished at an angle of 90° with a micropipet beveler (Model BV-10, Sutter Instrument Co.), first on 1200-grit sand paper and then on an extrafine diamond abrasive plate, to produce a smooth

(33) Oldham, K. B. *J. Electroanal. Chem.* **1988**, *250*, 1.
(34) Oldham, K. B. In *Microelectrodes: Theory and Applications*; Montenegro, M. I., Queiros, M. A., Daschbach, J. L., Eds.; Kluwer: Amsterdam, 1991; p 83.

carbon surface. Electrical contact to the carbon fiber was made by filling the top of the tube with mercury and inserting a stainless steel wire.

The carbon microcylinder was then coated in a manner similar to the microdisk tips. The tip of the microelectrode was pushed into a 1–2-μL drop of the coating solution using a micromanipulator. The mixture was allowed to rise into the glass pipet and coat the fiber. After the mixture dried, the end of the glass micropipet was blocked by the redox polymer film. Again, the film was cured at ambient temperature in air for a minimum of 2 days.

Antimony microdisk electrodes for the measurement of pH near electrode surfaces with the SECM were prepared from antimony shot as described previously.[10] The pH response of each electrode was calibrated using a glass electrode (Orion Research, Model 701A, Boston, MA) in phosphate buffers. The sensitivity of the electrodes was ~50 mV/pH unit, which is typical for polycrystalline antimony.[35]

Platinum microdisk electrodes used for comparison were prepared by sealing platinum wire (Goodfellow Metals Ltd., Cambridge, UK) in glass as described previously.[4] The reference electrode was a silver quasi-reference electrode (AgQRE).

Immobilized Glucose Oxidase. Glucose oxidase was immbolized on a carbon surface using a technique similar to the tip preparation above. The enzyme, redox polymer, and cross-linker [poly(ethylene glycol) (MW 400) diglycidyl ether] were mixed in a weight ratio of 3:7:0.5, and a drop of the solution was applied to the surface of a 3-mm-diameter carbon disk electrode. The mixture was allowed to cure in air at ambient temperature for ~2 days.

Instrumentation. The basic SECM instrument used in this work has been described in detail previously.[36] Briefly, a CE-1000 micropositioning device (Burleigh Instruments, Fishers, NY), connected to a PC via a DAC, controlled the movement of three piezoelectric inchworm motors. The tip was mounted on a three-axis translation stage and could be moved with submicron distance resolution under the control of the PC. The potentials of the tip and, when necessary, the substrate were controlled by a four-electrode EI-400 bipotentiostat (Ensman Instrumentation, Bloomington, IN). The tip and substrate currents were digitized and acquired by the PC using software written in-house (by D. O. Wipf).

Admittance–impedance measurements at UME tips in the SECM were made with a lock-in amplifier (Princeton Applied Research, model 5206, Princeton, NJ). The oscillator output of the lock-in was connected directly to the substrate or to a platinum or silver/silver chloride auxiliary electrode. The tip was held at virtual ground, and the current was measured with a high-frequency current follower. The real and imaginary components of the tip current as measured by the lock-in amplifier were fed into the ADC and collected by the PC.

A high-impedance buffer[10] was used for potentiometric SECM measurements with antimony pH-sensing tips. To avoid problems arising from the interaction of the ground of the EI-400 bipotentiostat and the ground of the high-impedance buffer, the substrate electrode was connected to channel B of the bipotentiostat and an external potential source (PAR 173 potential programmer) was used to run cyclic voltammograms. In this configuration, the reference electrode was at virtual ground and the potential of the tip could therefore be measured with respect to the same reference electrode used by the bipotentiostat. Tip potential and substrate current data were acquired simultaneously by the PC using the SECM software.

Cell and Substrate Electrodes. The cell (volume ca. 4 mL)[10,29] was machined from Teflon material, and the base was threaded to allow easy removal and exchange of different cell bases containing various substrate electrodes.

Glassy carbon substrate electrodes were made by heat-sealing 3-mm-diameter rod directly into a Teflon cell base using standard techniques. Gold substrate electrodes were made by first sealing 450-μm-diameter wire in 2-mm-o.d. soft glass capillaries under vacuum, polishing to expose a cross section, and then inserting them into a hole drilled in the cell base.

Chemicals. Peroxidase (EC 1.11.1.7; Type II, 200 units/mg of solid) from Horseradish (Sigma Chemical Co., St. Louis, MO) and glucose oxidase (EC 1.1.3.4; 122 units/mg of solid) from *Aspergillus niger* were used as received. The cross-linking agent [poly(ethylene glycol) (MW 400) diglycidyl ether] was obtained from Polysciences, and the redox polymer, [poly[(vinylpyridine)-osmium(bipyridine)$_2$Cl] derivatized with bromoethylamine] shown in Figure 1, was synthesized as previously reported.[37] Antimony shot (99.999%) was obtained from Aldrich. Fresh solutions of hydrogen peroxide were made up for each experiment by dilution of a concentrated commercial aqueous solution (30% by volume, Merck). The concentration of the commercial solution was checked by measuring the density. All other reagents were purchased from Aldrich or Sigma.

SECM Experimental Procedure. In general, the experimental procedure involved bringing the biosensor tip close to the sample surface and establishing the distance scale from the solution resistance (type A tips) or by deliberately touching the surface with the tip (type B tips).

For type A tips, the distance calibration was performed in 1 mM KCl. The in-phase and quadrature components of the current were monitored at a frequency of 10 kHz as the tip was pushed toward the surface. The tip was stopped when the real component had decreased by a factor of roughly 2. The tip was then withdrawn a known distance, disconnected from the lock-in amplifier, connected to the bipotentiostat, and held at a potential of −0.1 V vs AgQRE to detect peroxide. Fresh pH 7 phosphate buffer was usually added to the cell at this stage. The tip could then be pushed toward the surface to any desired tip-to-surface separation for imaging or electrochemical generation–detection experiments.

For type B tips, the tip was positioned as close as possible to the surface (~0.1 mm) using a telescopic lens. Next, the tip was connected to the bipotentiostat and very slowly (<0.5 μm/s) pushed toward the surface until a sudden jump in the current indicated that part of the tip was touching the surface. In some experiments, generation of a concentration profile of hydrogen peroxide at the surface aided this step. A gradual increase in tip current due to detection of peroxide was observed as the tip approached the surface, the tip approach was then continued at a slower rate until a sudden increase in the tip current was assumed to indicate electrical contact between tip and surface, and this point was taken as zero tip-to-surface separation. The tip was then withdrawn to the required distance for imaging or electrochemical experiments.

For potentiometric SECM experiments with antimony tips, the antimony tip potential was poised at a value where reduction of oxygen is diffusion controlled, and a current–distance curve corresponding to the case of an insulating substrate was recorded as reported previously.[10] The antimony tip was then reoxidized by returning the tip potential to 0 V for a few seconds to restore the pH function. The tip could then be connected to the high-impedance buffer for potentiometric measurements.

RESULTS

Characterization of Tips. Figure 3 shows a current–concentration calibration for a type B tip. A linear dependence of current on hydrogen peroxide was found up to ~100 μM (inset). If the active area of the tip is taken as roughly the same as the cross-sectional area of the end of the tip, a sensitivity of 0.75 A M^{-1} cm^{-2} is obtained. This is in reasonable agreement with the value of 1 A M^{-1} cm^{-2} found for macroscopic electrodes based on the same enzyme and redox polymer;[38] the discrepancy is mainly due to the uncertainty in the correct value of the area to be used in the calculation. Type B tips exhibited a slowly decaying background current, probably due to the redox process of parts of the polymer in poor electrical communication with the carbon fiber. This current was of the order of 10 pA after a few minutes at the

(35) Glab, S.; Hulanicki, A.; Edwall, G.; Ingman, F. *Crit. Rev. Anal. Chem.* **1989**, *21*, 29.
(36) Wipf, D. O.; Bard, A. J. *J. Electrochem. Soc.* **1991**, *138*, 469.
(37) Gregg, B.; Heller, A. *J. Phys. Chem.* **1991**, *95*, 5976.
(38) Vreeke, M.; Maidan, R.; Heller, A. *Anal. Chem.* **1992**, *64*, 3084.

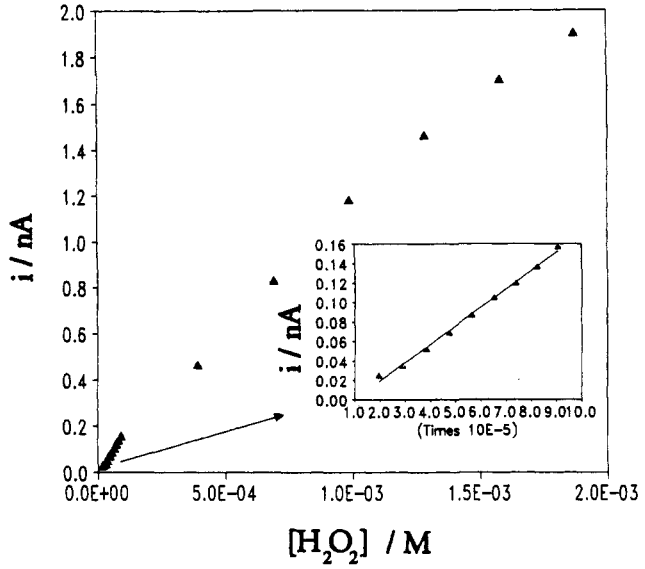

Figure 3. Current vs hydrogen peroxide concentration for a type B tip in 0.2 M pH 7 phosphate buffer. The inset shows the linear region below 100 μM.

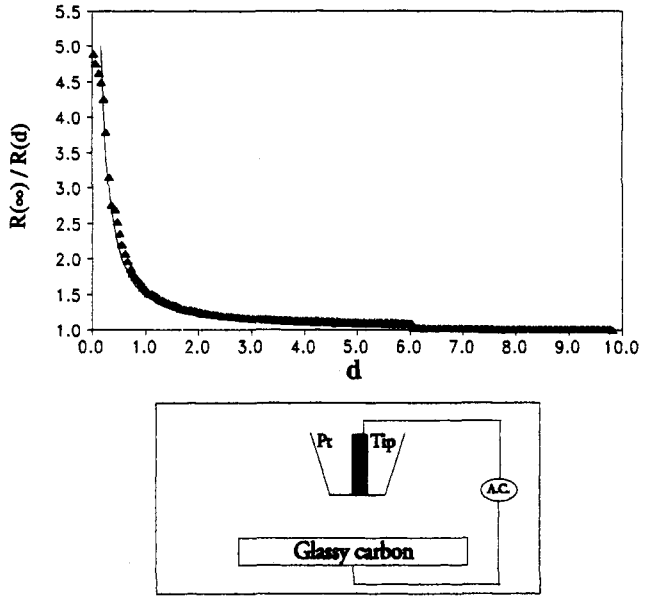

Figure 4. Conductance–distance curve for a 10-μm-diameter platinum UME over a glassy carbon surface in 1 mM KCl. Filled triangles are experiment and line is theory.

potential of −0.1 V vs AgQRE used for peroxide detection. Although type A tips showed smaller background currents, of the order of a few picoamperes, they produced ~10 times less current for a given concentration of peroxide. A crude estimate of the response time of the tips was made by monitoring the current on addition of peroxide to a stirred solution. Both type A and B tips showed similar response times, reaching 80% of the steady current in approximately 1–2 s; these values are close to those reported for glucose microelectrodes of similar design.[20]

Distance Calibration. Figures 4 and 5 show approach curves of conductance against distance for bare platinum UME tips over glassy carbon and Teflon substrates, respectively. These approach curves were recorded in a 1 mM KCl solution, since the UME double-layer capacitance dominates the impedance of the system in solutions of high ionic strength. Although the agreement with theory is excellent, this method of approaching the surface suffers from the limitation that as the tip becomes smaller, the double-layer capacitance decreases, and the relative contribution of the solution

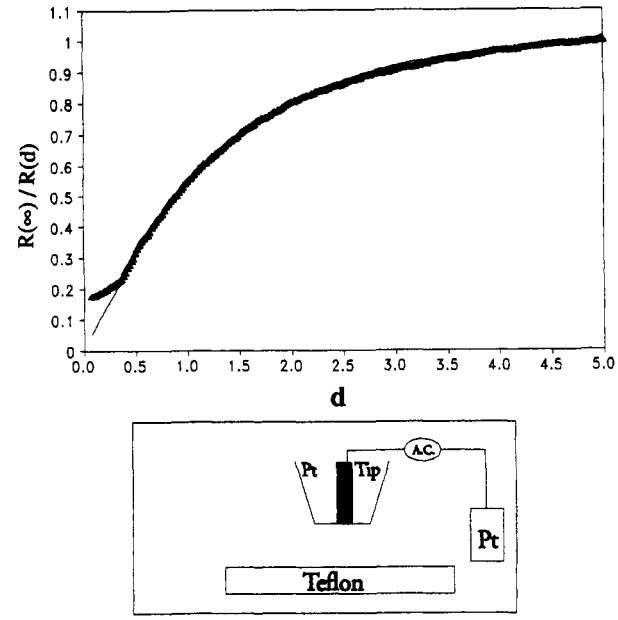

Figure 5. Conductance–distance curve for a 25-μm-diameter platinum UME over a Teflon surface in 1 mM KCl. Filled triangles are experiment and line is theory.

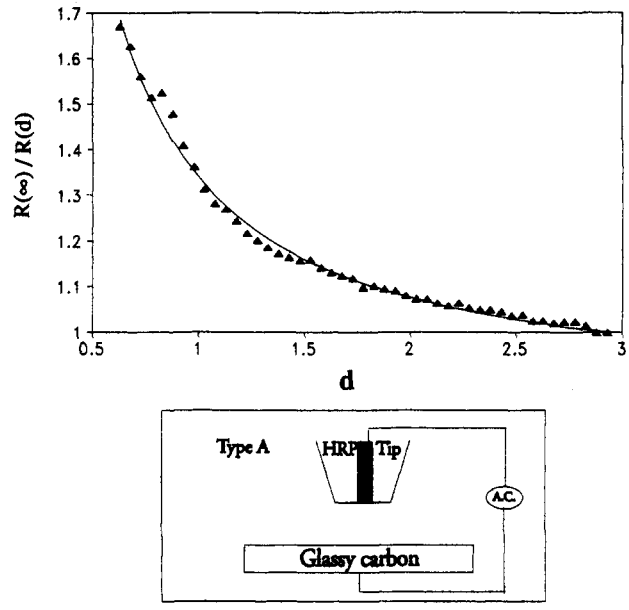

Figure 6. Conductance–distance curve for an 11-μm-diameter type A tip over a glassy carbon surface in 1 mM KCl. Filled triangles are experiment and line is theory.

resistance to the impedance decreases. Moreover, the method of data analysis outlined in the theory section depends on the assumption of a simple RC series equivalent circuit, i.e., with no faradaic process. To some extent these problems can be overcome by the use of low-conductivity solutions and high frequencies so that the contribution of the solution resistance to the impedance is maximized.

The advantage of this method is that it works equally well for insulating and conducting surfaces and could even be used to distinguish regions of different conductivity on a surface in exactly the same way as amperometric SECM. A further advantage is the relative insensitivity to the presence of a thin polymer film on the tip. This is shown in Figure 6, the approach curve for a type A biosensor tip over a glassy carbon surface. The agreement with theory is still sufficiently good to allow calibration of the tip-to-surface distance with an accuracy better than 1 μm. The presence of the polymer film on the tip increased the measured capacitance by a factor of

Table 1. Pathways of Electrochemical Reduction of Oxygen

	reaction	electrode potential/V vs NHE[18]
a	$O_2 + 2H_2O + 4e^- \rightarrow 4OH^-$	+0.401
b	$O_2 + 4H^+ + 4e^- \rightarrow 4H_2O$	+1.229
c	$O_2 + H_2O + 2e^- \rightarrow HO_2^- + OH^-$	−0.065
d	$HO_2^- + H_2O + 2e^- \rightarrow 3OH^-$	+0.867
e	$O_2 + 2H^+ + 2e^- \rightarrow H_2O_2$	+0.67
f	$H_2O_2 + 2H^+ + 2e^- \rightarrow 2H_2O$	+1.77
g	$2H_2O_2 \rightarrow 2H_2O + O_2$	catalyt decomp

~2, possibly due to a change in effective area. No significant difference in resistance between coated and uncoated tips was observed, and therefore, no correction for this was applied. The signal-to-noise ratio for coated electrodes in resistance measurements was poorer than for uncoated ones for reasons that are not clear.

Unfortunately, although type A tips could easily be positioned close to a surface using this method, only ~10% of these tips functioned well as biosensors. The reason for this was the poor adhesion of the polymer to the glass. The swelling of the polymer in solution often resulted in loss of polymer from the tip. For this reason, type B tips were constructed and were found to function as biosensors much more reliably. However, the geometry of these tips does not allow the use of the above theory for the conductance–distance measurement. Instead, the distance was determined by deliberately touching the tip to the conductive surface as described in the Experimental Section. Although this method could be used to calibrate a conductance–distance curve, it was carried out with the tip under potentiostatic control for convenience. This method of distance calibration has several disadvantages, the most obvious being the possibility of damaging the tip, and indeed, it was necessary to use very slow scan rates, 0.5 μm/s or less, when approaching the substrate. Moreover, this method only works with conductive substrates.

Electrochemical Reduction of Oxygen. The mechanism of the electrochemical reduction of oxygen has been intensively studied.[23,24] The reaction is complex, because it involves multiple electron- and proton-transfer reactions and proceeds through a series of high-energy intermediates, e.g., $O_2^{\bullet-}$, and $HO_2^{\bullet}$, with the more stable intermediate H_2O_2 also frequently formed. In aqueous solution, the mechanism depends on electrode material, pH, electrode potential, electrode pretreatment, and purity of the system.[24,39] A few of the processes often found in the main overall reduction are shown in Table 1. Reactions of radical intermediates such as $OH^{\bullet}$, $O_2^{\bullet-}$, and $HO_2^{\bullet}$ are not considered because their lifetimes are too short in aqueous solution to be detected in the SECM experiments reported here. Rotating ring–disk studies have demonstrated the presence of hydrogen peroxide as a stable intermediate.[23,24,39-43] These investigations have shown that, on most electrode materials (other than platinum), the hydrogen peroxide pathway (c–f) accounts for essentially all the current. On platinum electrodes in acidic solutions at low overpotentials, no hydrogen peroxide is detected, leading to the proposal that oxygen is reduced to water without a peroxide intermediate (b) perhaps via dissociative adsorption of oxygen.[23] Alternatively, the intermediates ($O_2^{\bullet-}$, $HO_2^{\bullet}$, or peroxide) may be strongly adsorbed on the surface and reduced to water before they desorb.[24] Furthermore, platinum is known to catalyze the disproportionation of hydrogen peroxide to water and oxygen (g), and therefore, it has been suggested that the rate of hydrogen peroxide decomposition is as fast as its rate of formation. With gold and glassy carbon electrodes, however, hydrogen peroxide is formed as a stable intermediate at any pH.[42,43] Parts A and B of Figure 7 illustrate the results of substrate generation–tip detection experiments using a peroxide-sensing UME tip close to carbon and gold substrate electrodes reducing oxygen in phosphate buffer solutions. The tip potential (with a type A or type B tip) was held constant at −0.1 V vs AgQRE (ca. +0.1 V vs SCE) to detect hydrogen peroxide, and the substrate potential was slowly swept into the region where oxygen is reduced. As the substrate begins to reduce oxygen, for both electrodes at potentials more negative than ca. −0.3 V, the tip current rises because of detection of hydrogen peroxide in the diffusion layer. Eventually, the tip current decreases again as the substrate potential becomes sufficiently negative to reduce the hydrogen peroxide to water. This is clearly seen in the case of glassy carbon (Figure 7A), where two separate, drawn-out waves are seen in the forward scan of the substrate voltammogram corresponding to potentials where the tip current rises and falls. The rise in peroxide detection current on the reverse scan occurs at roughly the same potential (−1 V) as the fall in tip current on the forward scan, confirming the identification of the two waves in the substrate voltammogram as the reduction of oxygen to peroxide and reduction of peroxide to water, respectively. This also shows that the decrease of the peroxide detection current on the forward scan reflects a potential-dependent process and is not due to a slow, time-dependent process, e.g., catalytic decomposition. The time lag for the rise of the tip current on the reverse scan is due to the slow diffusion of oxygen from the bulk solution to the carbon surface, and the slow decay of the tip current at the end of the reverse scan is due to the relaxation of the concentration profile of hydrogen peroxide between the carbon surface and the bulk solution. These results demonstrate that the tip is functioning and are in agreement with previous rotating ring–disk studies on carbon electrodes.[23]

In the case of gold (Figure 7B), the process is more complex. On the forward (0 to −1.7 V) scan, the tip current rises because of the reduction of oxygen to peroxide beginning at ~−0.2 V on the gold substrate (inset on substrate voltammogram). As with carbon, the decrease in tip current at −1.0 V is due to reduction of peroxide to water. The wave for the reduction of peroxide cannot be distinguished on the Au voltammogram, because it merges with the large reduction wave (discussed below) attributed to buffer reduction. However, the tip current does not decrease to zero, but plateaus at ~18 pA beginning at −1.2 V, indicating that peroxide reduction on the gold surface is blocked. Two plausible explanations for this behavior are fouling of the electrode surface or a shift to higher pH at the gold surface, which could reduce the rate of reduction of peroxide. To test this, the pH near the gold surface was directly measured using an antimony tip under the same conditions (Figure 7C). The small apparent rise in pH at −0.3 V in Figure 7C is due to depletion of oxygen, which causes the rest potential of antimony to become more negative. Despite this interference, Figure 7C clearly shows that the pH increases significantly only at potentials more negative than ~−1.5 V (where water reduction occurs) and therefore cannot account for the blocking of peroxide reduction at −1.2 V in Figure 7B. This sharp pH increase does, however, account for the drop in peroxide detection current at −1.5 V, which

(39) Damjanovic, A.; Genshaw, M.; Bockris, J. O'M. *J. Chem. Phys.* **1966**, *45*, 4057.
(40) Damjanovic, A.; Genshaw, M.; Bockris, J. O'M. *J. Electrochem. Soc.* **1966**, *113*, 1107; **1967**, *114*, 466.
(41) Muller, L.; Nekrasov. *J. Electroanal. Chem.* **1965**, *9*, 282.
(42) Genshaw, M. A.; Damjanovic, A. Bockris, J. O'M. *J. Electroanal. Chem.* **1967**, *15*, 163.
(43) Tarasevich, M. R.; Subirov, F. Z.; Mertsalova, A. P.; Burstein, Kh. *Electrokhim.* **1968**, *4*, 432, **1969**, *5*, 608; **1970**, *6*, 1130.

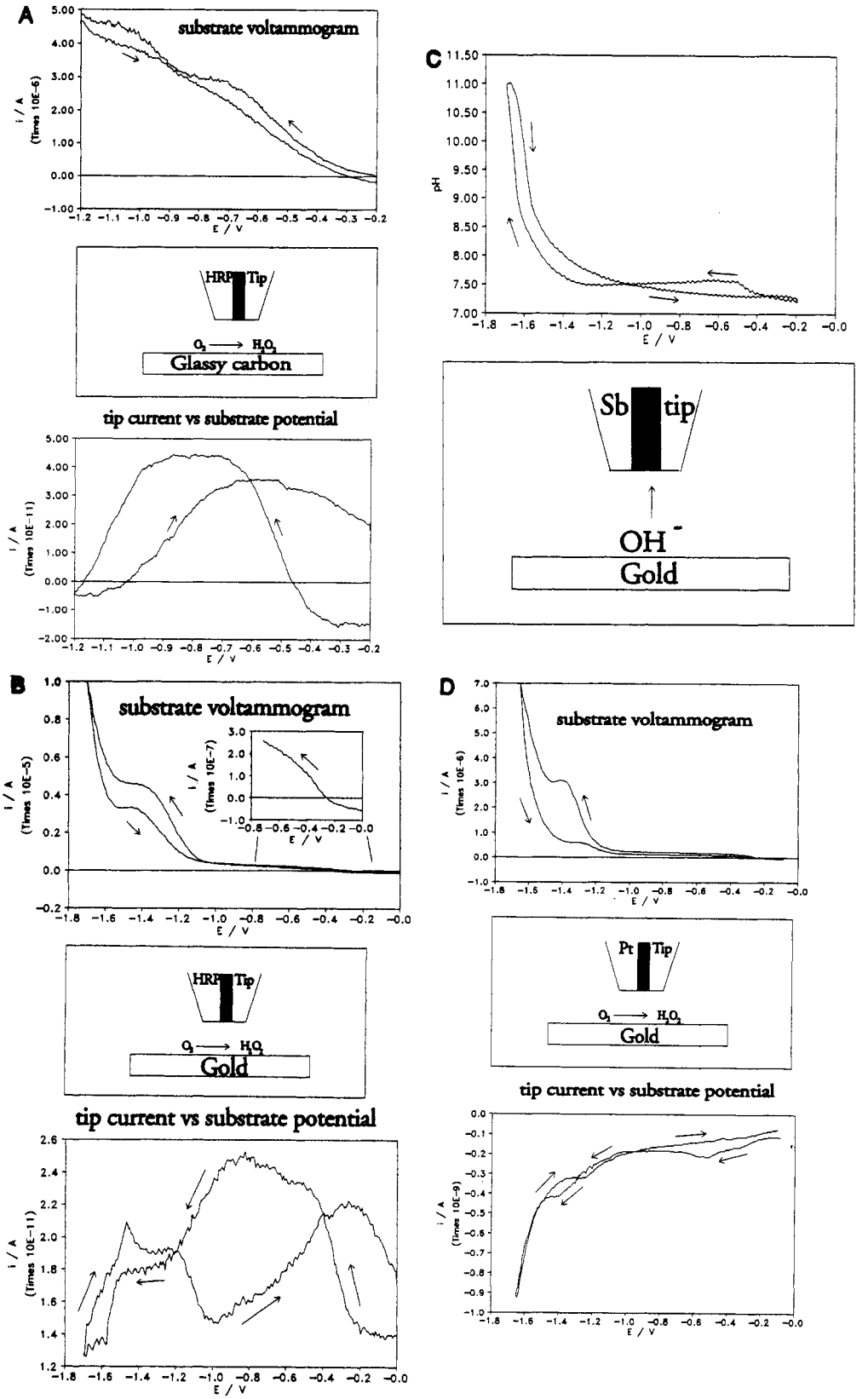

Figure 7. (A) Tip (type A) and substrate (glassy carbon) current as a function of substrate potential during a scan (2 mV/s) with a tip-to-surface distance of 10 μm. (B) (Tip) (type B) and substrate (gold) current as a function of substrate potential during a scan (10 mV/s) with a tip-to-surface distance of $\sim$10 μm. The inset shows the oxygen reduction wave on the forward scan. (C) Tip (20-μm-diameter antimony) potential and substrate (gold) current as a function of substrate potential during a scan (10 mV/s) with a tip-to-surface distance of 10 μm. (D) Tip (10-μm-diameter platinum at +0.7 V) and substrate (gold) current as a function of substrate potential during a scan (10 mV/s) with a tip-to-surface distance of 10 μm. Solutions contained air-saturated 0.2 M pH 7 phosphate buffer, and the reference electrode was a silver wire.

is likely due to deactivation of the enzyme at such a high pH. The pH dependence of a macroscopic horseradish peroxidase electrode is consistent with this interpretation (Figure 8). The peroxide detection current is roughly independent of pH in the range 4.5–7.5. Outside this range, however, the enzyme is deactivated, losing 90% activity by pH 10.5 but recovering on returning to lower pH. The plateau in the tip current in the potential range −1.2 to −1.5 V (Figure 7B)

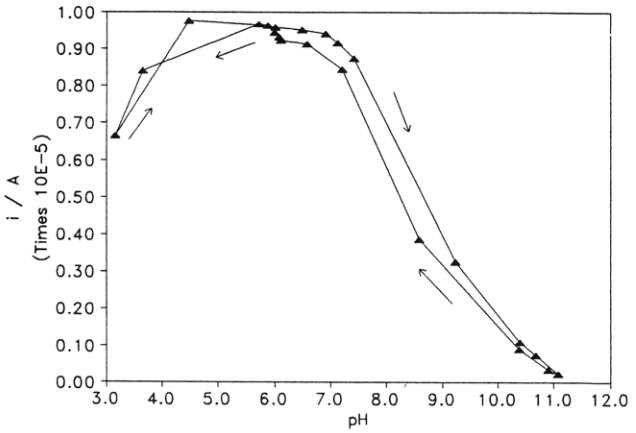

Figure 8. pH dependence of a macroscopic horseradish peroxidase electrode. The electrode used was a 3-mm-diameter glassy carbon disk coated with horseradish peroxidase in redox polymer **1**. The solution contained 0.12 mM hydrogen peroxide, and the electrode potential was 0 V vs SCE.

corresponds to the large reduction wave on the gold substrate. This wave is absent in solutions containing only KCl as electrolyte, but appears on addition of phosphate buffer and is therefore attributed to reduction of buffer anions (e.g., $H_2PO_4^-$) to hydrogen. It is tentatively suggested that the electrode becomes fouled by adsorbed species produced by this reaction and that this inhibits the reduction of peroxide in this potential range, although other mechanisms cannot be ruled out on the basis of the available data. A similar effect has been reported for the reduction of hydrogen peroxide on germanium, and the decrease in reaction rate was interpreted as being due to the adsorption of hydrogen atoms on the active sites for peroxide reduction.[44] During the reverse scan in Figure 7B, the current rises in the range −1.0 to −0.3 V because the potential is no longer sufficient to reduce peroxide, and finally, the tip current falls again at potentials greater than −0.3 V, where oxygen is not reduced, because of diffusion of peroxide away from the surface to the bulk solution. For comparison, the experiment was repeated using a platinum UME as a detector, as shown in Figure 7D. The platinum tip, held at a potential where H_2O_2 oxidation occurs, responds to the production of hydrogen peroxide, but at potentials corresponding to the reduction of the buffer or water; the peroxide detection current is obscured by a large anodic current due to oxidation of hydrogen produced by these processes. The increase in detector current seen at ∼−1.2 V confirms the identification of the large plateau in the substrate current at −1.2 to −1.5 V in Figure 7B as the reduction of buffer anions to hydrogen and also demonstrates the selectivity advantage of the biosensor tip, which is almost insensitive to the presence of hydrogen.

Imaging Catalytic Activity. In addition to being a tool for studying reaction mechanisms, SECM can be used to image catalytic activity. This is demonstrated for two systems. Figure 9 shows an image of the hydrogen peroxide detection current over an unbiased platinum microdisk in a solution of hydrogen peroxide. The glass insulator is inert to peroxide, but the platinum surface catalyzes the disproportionation of hydrogen peroxide to oxygen and water, as in Table 1g above. Far from the platinum disk, the peroxide concentration is constant, but decreases as the tip moves over the region near the platinum surface. The image is elongated in a direction perpendicular to the scanning motion of the tip. A possible explanation of this is that the sample surface is tilted with respect to the plane in which the tip was scanned. This results in the tip observing an elliptical section of the concentration

(44) Gerischer, H.; Mindt, W. *Surf. Sci.* **1966**, *4*, 440.

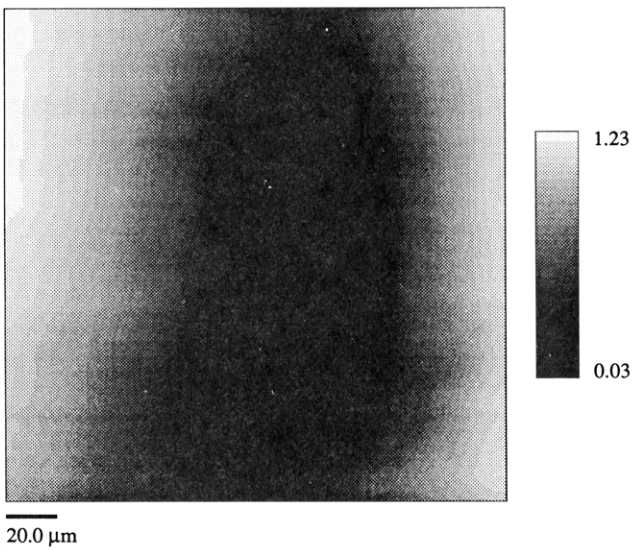

Figure 9. Image of the concentration profile of hydrogen peroxide around a 25-μm-diameter platinum microdisk in a solution of 0.88 mM hydrogen peroxide and 0.2 M pH 7 phosphate buffer.

profile around the disk. This image was taken with a type B tip, and the poor orientation of the tip and surface could only be avoided by making multiple tip crashes for distance determination. Obviously this procedure is not satisfactory. However, the response of type B tips to peroxide was more stable, and nearly all type B tips prepared had a usable response to peroxide, whereas type A tips did not show a stable response to peroxide for the long periods of time (30 min to 1 h) required to collect these images. Despite the lack of a completely satisfactory distance calibration, type B tips could be used in a qualitative way to image catalytic activity. Figure 10A is an image of the distribution of hydrogen peroxide in the diffusion layer of a glassy carbon electrode which was partially covered with platinum. This surface was prepared by electrodepositing platinum onto a 3-mm-diameter glassy carbon disk from a solution of hexachloroplatinic acid in 0.1 M HCl at a potential of −0.5 V vs Ag/AgCl. This resulted in an uneven distribution of platinum islands partially covering the surface. The platinum deposit was cleaned by potential cycling in 0.5 M H_2SO_4 until the characteristic hydrogen adsorption–desorption peaks were obtained. The dark area in Figure 10A (low tip current) shows a region covered with platinum where oxygen and hydrogen peroxide are reduced to water. The light area is the bare carbon surface where peroxide is a stable intermediate in the reduction of oxygen. A small dark spot visible in the upper right-hand corner of the image suggests the presence of a small, ca. 10-μm, platinum particle. Figure 10B shows an optical micrograph of the surface; unfortunately, it was not possible to determine the part of Figure 10B scanned in Figure 10A because of the lack of structure in the SECM image. However, a comparison with the optical micrograph of the surface shows an important aspect of the technique, that only isolated sinks (or sources) can be resolved. The main platinum region is composed of smaller islands that are so close together that their diffusion layers overlap and are not distinguished in Figure 10A. This limitation is inherent to versions of SECM relying on generation of an electroactive species by the surface under study[10] and to fluorescence imaging[30] where a fluorescence-inducing species is generated, but is less important in feedback SECM experiments where the resolution is determined only by the tip size.[7,8] In comparison with fluorescence imaging, the imaging technique with the enzyme electrode is very slow, requiring 30 min or more to scan a 300-μm by 300-μm region. This is due to the relatively slow, 1–2 s, response time of the

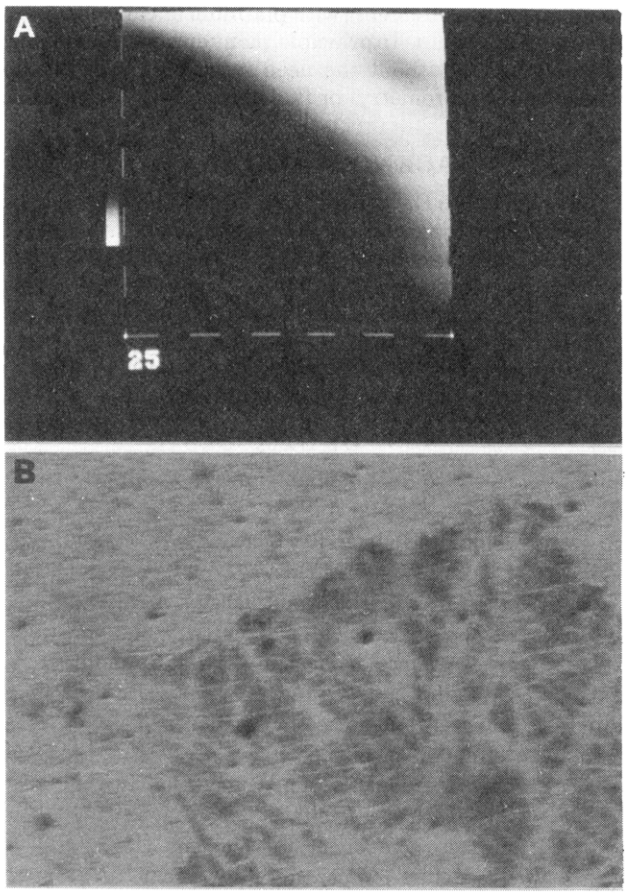

Figure 10. (A) Image of the concentration profile of hydrogen peroxide near the surface of a glassy carbon–platinum composite. The solution contained air-saturated 0.2 M pH 7 phosphate buffer, and the potential of the glassy carbon substrate was −1.0 V vs AgQRE. The tip to surface distance was ~20 μm. The white scale bars indicate 25 μm. (B) Optical micrograph of the surface of the glassy carbon–platinum composite from (A). The photograph shows an area ca. 500 μm across. Darker areas are electrodeposited Pt.

tips which necessitates the use of scan rates of 5 μm/s or less. However, the technique does have the ability to provide concentration profiles normal to the surface instead of integrating over a light path.

Enzymatic Oxygen Reduction. Hydrogen peroxide is formed in several oxidase-catalyzed oxidations of substrates by oxygen.[28] A simplified scheme for glucose oxidation catalyzed by glucose oxidase is shown below:

$$GO_{OX} + \beta\text{-D-glucose} \rightarrow GO_{red} + \text{D-gluconolactone} \quad (15)$$

$$GO_{red} + O_2 \rightarrow GO_{ox} + H_2O_2 \quad (16)$$

Therefore an attractive possibility for assaying enzyme activity on a small (length) scale is the measurement of the hydrogen peroxide produced. This is easily done using the peroxide-sensing tips described here. Glucose oxidase was immobilized on a glassy carbon disk (ca. 3-mm diameter) by trapping in the same polymer as used for the tip. The immobilized glucose oxidase was placed in air-saturated pH 7.0 phosphate buffer and 1 mM glucose was added. After allowing the enzyme to generate hydrogen peroxide via reactions 15 and 16 for a few minutes, a quasi-steady-state concentration profile of hydrogen peroxide developed at the surface of the carbon disk. Figure 11 shows an approach curve of tip current against distance over immobilized glucose oxidase in a solution of glucose. The tip current rises slowly over a distance of several hundred micrometers because of

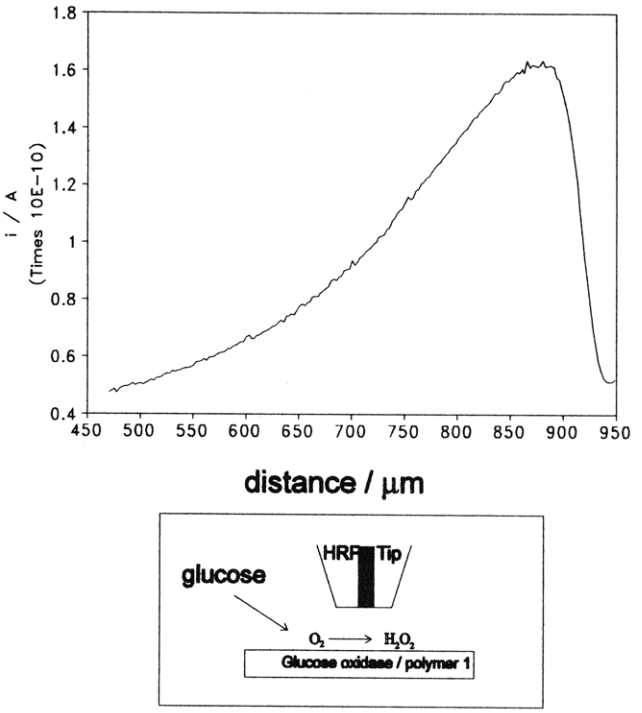

Figure 11. Current–relative distance curve for a type B tip approaching the surface of a glassy carbon disk coated with immobilized glucose oxidase. The solution contained 1 mM glucose and air-saturated 0.2 M pH 7 phosphate buffer. The whole approach curve (limited by the maximum piezo travel of ~475 μm) is shown.

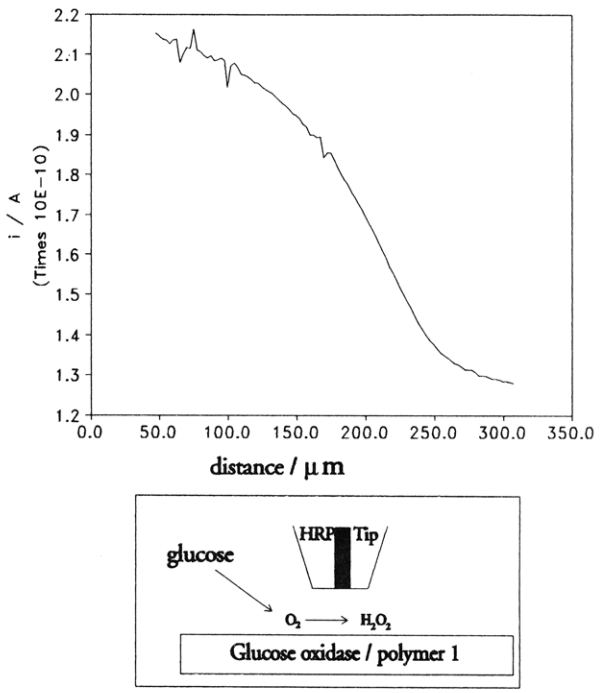

Figure 12. Line scan across the edge of an immobilized glucose oxidase layer. At distances greater than ca. 300 μm, the tip is above a bare carbon surface. The solution contained 1 mM glucose and air-saturated 0.2 M pH 7 phosphate buffer.

the large size of the carbon disk used as substrate. The sharp decrease in tip current is due to the tip blocking diffusion of glucose and oxygen to the immobilized glucose oxidase on the carbon surface under the tip when the tip is close to the surface; the small increase that follows may indicate the tip touched the surface. On scanning the tip over the middle of this surface (not shown), the measured peroxide concentration was constant within ~10%, indicating that, with the proviso

discussed in the previous section, the distribution of enzyme in this polymer is quite uniform, in contrast to the observations of Wang and co-workers for the case of glucose oxidase trapped in polypyrrole.[45] Figure 12 shows a scan across the boundary of the polymer–enzyme-coated region and the bare carbon surface, where the current drops to a constant low value over a distance range of roughly 100 μm.

CONCLUSIONS

The utility of horseradish peroxidase microelectrodes in SECM has been demonstrated for mechanistic studies of oxygen reduction and for the detection of immobilized oxidases without the need for artificial redox mediators. For measurements of hydrogen peroxide in the diffusion layer, there are three main advantages over rotating ring–disk techniques. These are the excellent selectivity for hydrogen peroxide over other electroactive compounds, the high sensitivity, and the possibility of imaging distributions of catalytic activity on the surface. However, these sensors have a restricted useful pH range (ca. 4–8); moreover, the substrate generation–tip detection mode of operation is not convenient for quantitative measurements requiring a well-defined collection efficiency or for high-resolution imaging. The sensors have a relatively long response time, which restricts the scanning rate of the tip across the surface and hence increases the time required to obtain an image. This restricts the technique to imaging of steady-state concentration profiles. From the various studies carried out with the tip described here (see, e.g., Figure 10A), we judge the resolution attainable with this technique to be of the order of tens of micrometers.

The technique has promise in the study of enzymatic systems where the presence of many electroactive components could make measurements with platinum or carbon detector electrodes uncertain. In principle, many enzymatic oxidations can be studied without the need to add additional redox mediators (amperometry) or fluorescent dyes (fluorescence imaging).

(45) Yaniv, D. R.; McCormick, L.; Wang, J.; Naser, N. *J. Electroanal. Chem.* **1991**, *314*, 353.

ACKNOWLEDGMENT

The help of Dr. D. O. Wipf in building the high-frequency current follower is gratefully acknowledged. The support of our research by the Office of Naval Research, the National Science Foundation (CHE9214480), the Robert A. Welch Foundation, and the National Institutes of Health is also gratefully acknowledged.

Scientific Parentage of the Author. A. J. Bard, Ph.D. under J. J. Lingane, Ph.D. under I. M. Kolthoff.

LIST OF SYMBOLS

ϕ	electrostatic potential
j	current density, A cm^{-2}
κ	solution conductivity, S cm^{-1}
c	concentration, mol cm^{-3}
$i_T(d)$	SECM feedback current density, A cm^{-1}
D	diffusion coefficient, cm^2 s^{-1}
d	tip-to-surface distance in units of tip radius
a	tip radius, μm
$R(d)$	solution resistance as a function of d
c_{dl}	tip double-layer capacitance
ω	angular frequency of ac voltage
V	magnitude of ac voltage
$i_{0°}$	in-phase component of ac current
$i_{90°}$	quadrature component of ac current

RECEIVED for review June 28, 1993. Accepted September 28, 1993.[⊗]

[⊗] Abstract published in *Advance ACS Abstracts,* November 1, 1993.